

Supporting information

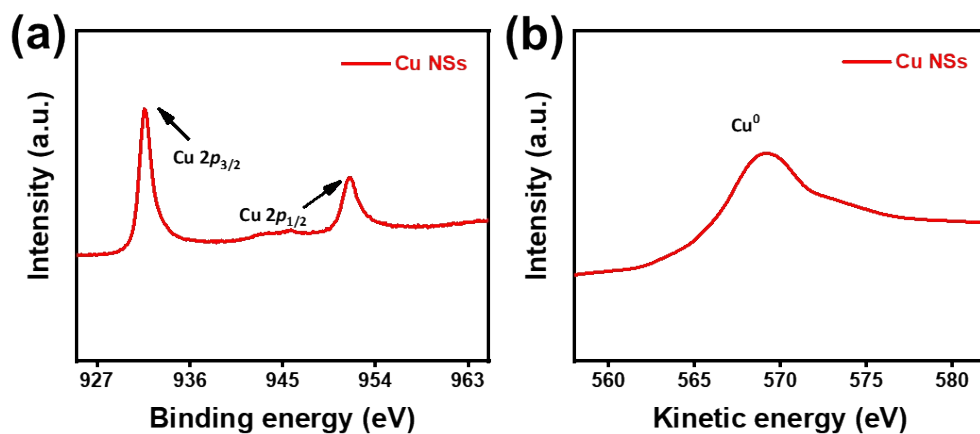


Fig. S1. The Cu 2p XPS spectra (a) and the auger electron spectrum of Cu LMM (b) of Cu NSs prepared by an *in-situ* electrochemical deposition method.

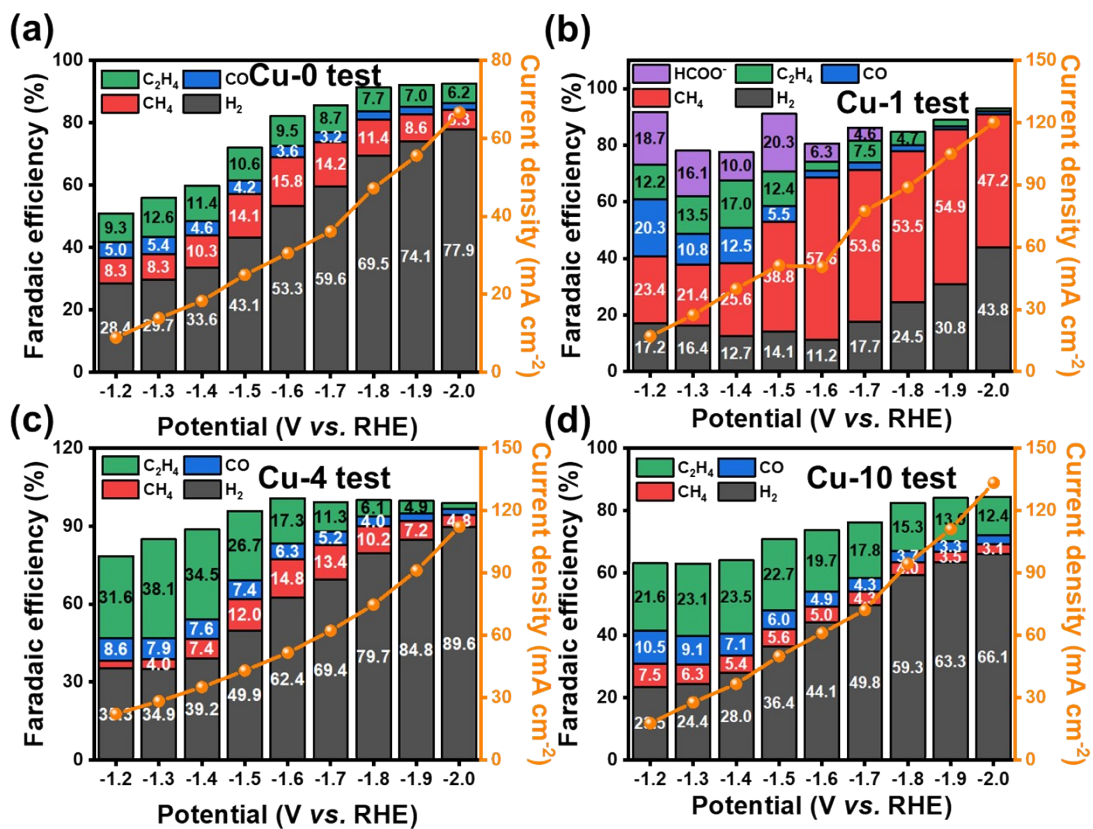


Fig. S2. The faradaic efficiency of Cu NSs under Cu-0 (a), Cu-1 (b), Cu-4 (c), and Cu-10 (d) test conditions after the electrochemical deposition for Cu NSs preparation in an H-type cell.

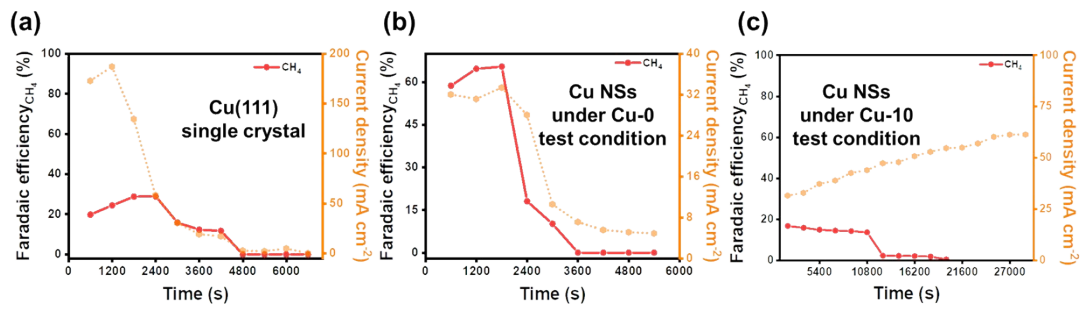


Fig. S3. The long-time faradaic efficiency stability tests of Cu(111) single crystal in 0.1 M KHCO₃ electrolyte (a) and Cu NSs under Cu-0 (b) and Cu-10 (c) test condition at -1.6 V vs. RHE.

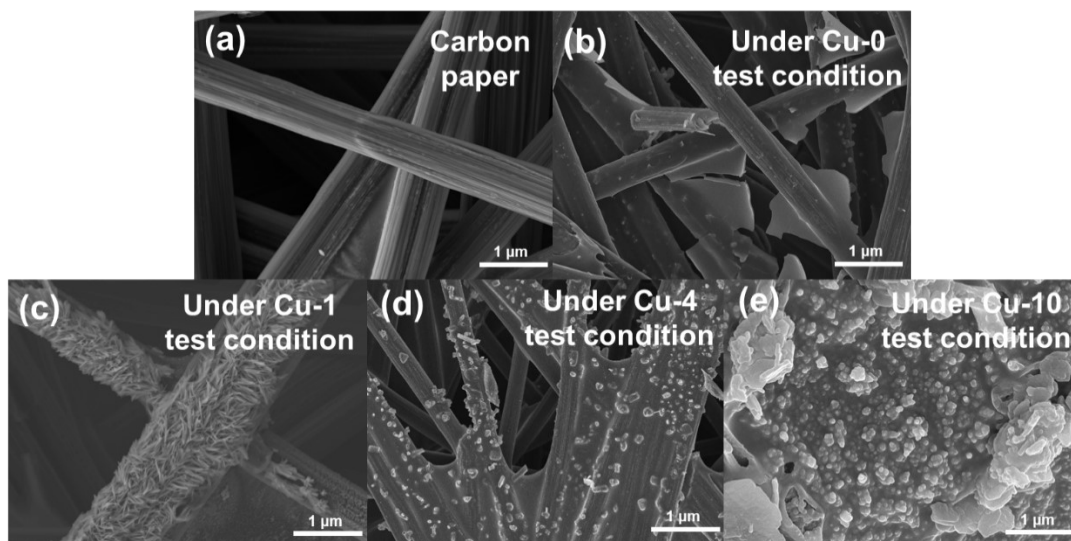


Fig. S4. The SEM images of the Carbon paper (a) and supported Cu catalysts after long-term performance test under Cu-0 (b), Cu-1 (c), Cu-4 (d), and Cu-10 (e) test conditions.

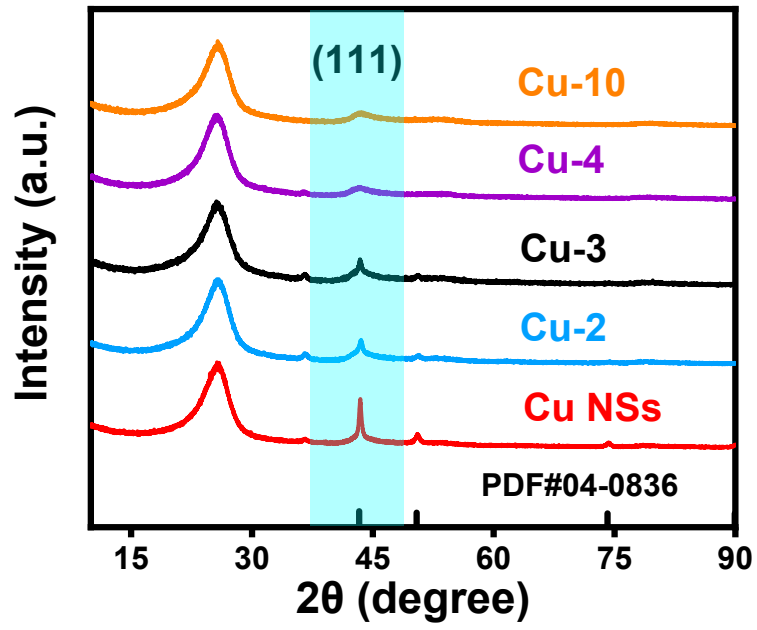


Fig. S5. The XRD patterns of Cu NSs in electrolytes with different Cu^{2+} content.

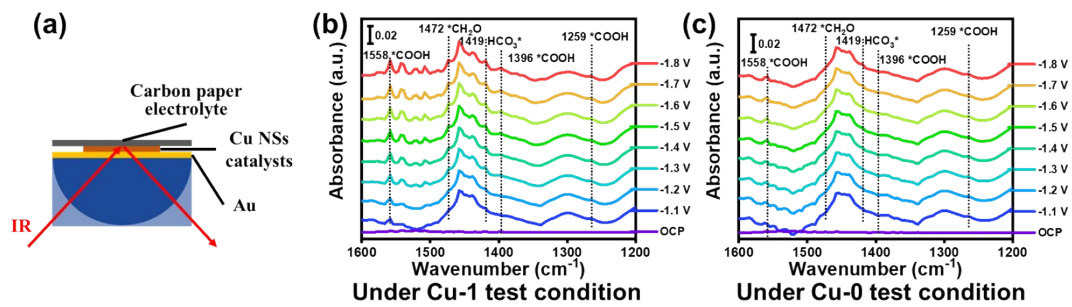


Fig. S6. (a) The test method of the *in-situ* FTIR experiments. The *in-situ* FTIR spectra of the Cu NSs under Cu-1 (b) and Cu-0 (c) test condition.

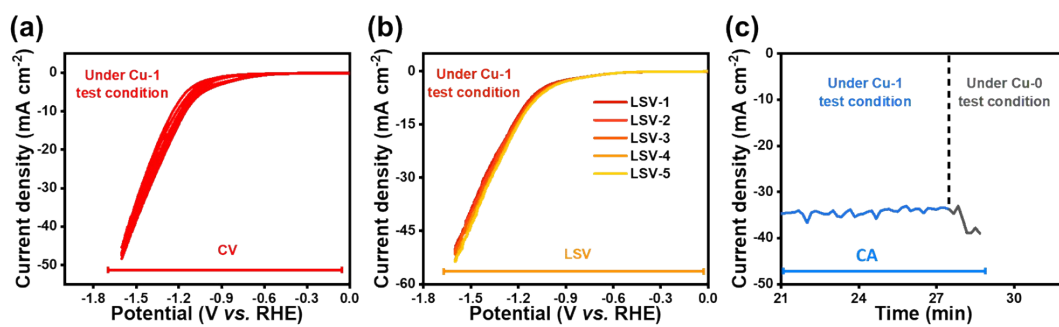


Fig. S7. The cyclic voltammetry (CV) curve, linear sweep voltammetry (LSV) curve and chronoamperometry (CA) curve during the *in-situ* EQCM-D tracking experiments.

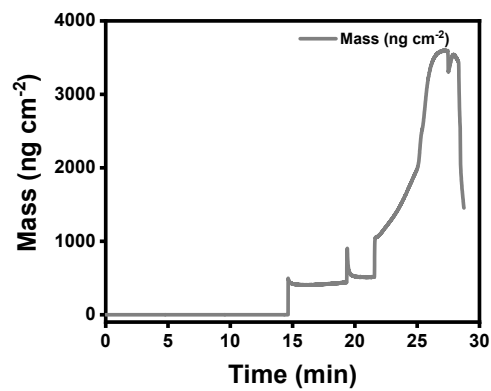


Fig. S8. The mass change under the condition of the chronoamperometry test after being transferred to Cu-0 test condition.